위험구간용 고규격 강재 방호울타리의 충돌 거동 및 보강 방법

Impact Performance of High Grade Steel Barrier for Hazardous Area and Strengthening Method

고 만 기[1] · 김 기 동[1]
Ko, Man Gi *Kim, Kee Dong*

요 약 : 최근 고속도로와 철도가 평행하게 달리는 경우와 같은 특정위험구간에 안정성과 동시에 좋은 시야를 확보하기 위하여 다양한 철재 베리어가 제안되어 설치되고 있다. 그러나 이러한 베리어 중에서 어느 것도 국내의 충돌조건 14tonf-80km/h-15° 을 만족시키는지 확실하게 검증된바가 없기 때문에 본 연구에서는 베리어 예비설계에 가장 많이 사용되고 있는 Barrier Ⅶ 프로그램을 사용하여 이러한 철재 베리어의 충돌거동을 조사하였다. 해석결과 조사된 베리어 모두 필요한 강성을 발현하지 못하였고 유형 C베리어의 강성이 상대적으로 우수하였다. 따라서, 기 시공된 유형 C 가드레일을 보강하기 위한 방안을 실험적으로 검토하였고 지주에 콘크리트를 부분적으로 충전하여 보강하는 방법이 충돌조건을 효율적으로 만족시킬 수 있음을 확인하였다.

ABSTRACT : To secure good visibility various steel flexible barriers were introduced and constructed in the area where a highway runs in parallel with a railroad. However, none of the flexible barriers was proven to satisfy the performance criteria for the impact condition of 14tonf-80km/h-15° set forth by Korea design guide. Thus, in this study, the impact performance of the flexible barriers was investigated by using Barrier Ⅶ program, which was most widely used for the preliminary design of barriers. From the analytical results, it has been found that none of the barriers satisfied the stiffness requirement while Type C barrier showed stiffer behavior than the others. Thus, the way to strengthen the installed Type C barrier was experimentally investigated. The method of partially filling concrete inside the post was efficient to satisfy the performance criteria for the impact condition of 14tonf-80km/h-15° .

핵 심 용 어 : 철재 베리어, 콘크리트 충전 지주, 지주실험, 충격조건, 베리어 VII
KEYWORDS : Steel Barrier, Concrete Filled Post, Post Test, Impact Condition, Barrier VII

1) 정회원, 공주대학교 조교수, 공학박사

본 논문에 대한 토의를 2001년 2월 28일까지 학회로 보내주시면 토의 회답을 게재하겠습니다.

1. Introduction

Recently, in Korea, to secure good visibility various steel barrier systems are introduced in a specific danger area such as a road which runs in parallel with a railroad, and some of them have already been constructed in that area. Among them typical three steel barriers are shown in Fig. 1. The main feature of these steel barriers is that they have two rails and 2m center-to-center post spacing while the general roadside barriers have one rail and 4m center-to-center post spacing. Type A and Type B barriers have W-beam section as a main rail while Type C barrier has thrie-beam section. Type B and Type C barriers have round shape section of 145×100×4mm size (guard beam) as upper rail while Type A barrier has W-beam section. As upper rail Type A barrier has been installed on the highway shoulder with high embankments while Type C barrier has already been constructed in the highway with which a railroad is running in parallel.

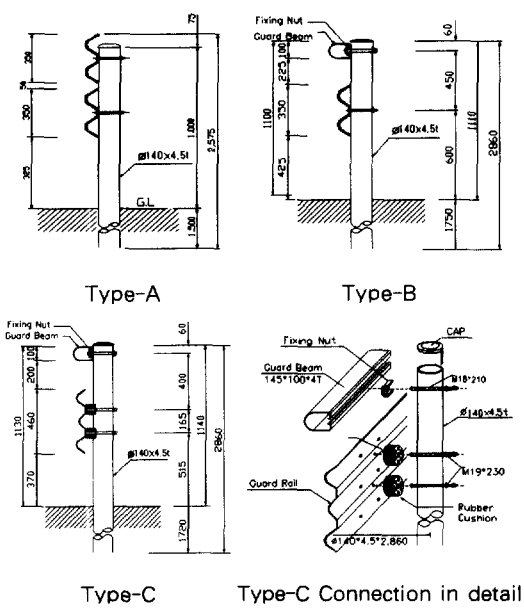

Fig. 1 Extra Grade Barrier Systems

However, none of the three systems was proven to satisfy the performance criteria set forth by Korea design guideline[1]. This raised a public concern on whether these systems can redirect impacting vehicles into a road without overriding or snagging in the highway with which a railroad is running in parallel. Korea design guideline classifies this kind of area as a specially dangerous region and recommends a very strong barrier system(Grade S). Impact condition to be required for the barrier system in this area is 14tonf-80km/h-15° . For this impact condition, the system should not deform larger than 110cm. This criterion is too high standard for a flexible barrier. Rigid system such as concrete barrier might be considered for this region. But, for the case that ensuring good visibility is an important factor, a flexible barrier can be an alternative. This research is therefore intended to evaluate the impact performance of the above three flexible systems and to recommend the best one. When none of the systems satisfies the impact condition, a way to improve the stiffness of the best one will be experimentally sought out. Evaluation is made through both simulations by Barrier Ⅶ program[2] and static tests.

2. Impact Simulation

Simulations for the above three flexible

barrier systems are conducted using Barrier Ⅶ.

Barrier Ⅶ program[2] is a widely used model for simulating impacts with flexible barriers. This program incorporates a beam and column finite element barrier model and a two dimensional vehicle model. The program incorporates both geometric and material non-linearities as well as a number of specialized barrier elements including nonlinear spring and dashpots. Although, the vehicle model incorporates relatively simple bilinear spring elements and is limited to three degrees of freedom, this program has been successfully validated for a wide variety of flexible barriers and a number of different vehicles. The primary limitation of this program is that it cannot be used to predict vehicle stability. However, the program is especially suited for use as a tool for barrier design in predicting maximum loads on and strains in barrier components. Further, the program has proven useful for identification of critical impact locations as well as predicting vehicle snagging and pocketing. Based on Korea design guide, the vehicle weight of 14tonf and impact angle of 15° are selected for the evaluation of structural adequacy.

Section properties and other input data for the beams and the posts of the flexible barriers shown in Fig. 1 are as shown in Tables 1 and 2. The yield forces and yield moments of beams shown in Table 1 are determined by using the specified minimum yield stress of SS400 steel. The post properties used for the Barrier Ⅶ simulations shown in Table 2 are the values idealized from post lateral force-displacement relations

Table 1 Section Properties of Beams

Beam Type	I (cm^4)	A (cm^2)	L (cm)	E (kPa* 10^8)	W (N/m)	Yield Force (kN)	Yield Moment (kN-m)
Thrie Beam	87	19.6	399.3	2.068	149.9	478.5	9.27
W-Beam	96	18.8	399.3	2.068	145.5	460.6	8.57
Guard Beam	492	17	399.3	2.068	130.8	416.9	19.52

Table 2 Section Properties of Posts

I (cm^4)	A (cm^2)	Stiffness (kN/cm)	Yield Moment (kN-cm)	Ultimate Shear (kN)	Deflection at Failure (cm)
440.1	19.2	9.76	1994.3	445	30

obtained by the pendulum test[5] and static test. The impact conditions for simulations are 14tonf-60km/h-15° and 14tonf-80km/h-15° . Two impact speeds are considered because the impact speed required for general roadside barriers is 60km/h and for barriers installed in specific danger area is 80km/h. In modeling the test vehicle the stiffnesses of 20tonf truck reported by PWRI[6] are applied to obtain the spring constants, which are required to model the vehicle body.

The simulation results of the three barriers for the two impact conditions are shown in Table 3. From the results, it can be seen that maximum longitudinal and lateral accelerations of the three barrier systems satisfy the acceleration index of 4g used for the assessment of occupant safety for the two impact conditions. For the impact condition of 14tonf-60km/h-15° , the maximum deflections of the three systems are smaller than the deflection limit of 1.1m used for the assessment of

structural adequacy while for the impact condition of 14tonf-80km/h-15° none of the systems satisfies the deflection limit of 1.1m. Among the three systems Type A barrier shows the most flexible behavior regardless of the impact condition. For the impact condition of 14tonf-60km/h-15° , the maximum deflection of Type C barrier is smaller than the others while for the impact condition of 14tonf-80km/h-15° the maximum deflection of Type B barrier is smaller. From the comparison of the deformed shapes of the three systems for the impact condition of 14tonf-80km/h-15° , it could be found that the barrier length, along which deflection was larger than the deflection limit of 1.1m, was smaller for Type C than for Type B. The barrier length violating the deflection limit was 2.36m for Type A, 2.19m for Type B and 1.97m for Type C.

From the computer simulations, it could not be clearly determined which one of Type B and Type C barriers was stiffer. Thus, to investigate which system had larger stiffness, static tests for the two systems were conducted. Since Type C barrier was the same as Type B barrier except that thrie-beam instead of W-beam was used as a main rail, the static tests were performed for the systems without upper rail. Figure 2 shows the test setup and the deformed shape of thrie-beam at the end of test. In Fig. 3 the load-deflection relations at beam center are shown. The ultimate strength of the system with thrie-beam(Type C) is 83.3 kN and that of the system with W-beam(Type B) is 51 kN. After beam stiffening occurs, the stiffness of Type C system is larger than that of Type B system while the stiffness of the two systems is

Table 3 Simulation Results

System	Impact* Condition	Maximum Deflection		Maximum long. acc.**		Maimum lat. acc.**	
		Def. (cm)	Time (s)	Acc. (g)	Time (s)	Acc. (g)	Time (s)
Type A (W Beam +W Beam)	I	93.5	0.75	-0.424	0.4	-1.122	0.25
	II	201.2	1.3	-1.022	0.7	-3.652	1.15
Type B (Guard Beam +W Beam)	I	89.4	0.75	-0.348	0.35	-1.107	0.35
	II	177.8	1.0	-0.473	0.55	-1.452	0.25
Type C (Guard Beam +Thrie Beam)	I	79.8	0.75	-0.348	0.35	-1.101	0.30
	II	187.9	1.4	-0.506	0.25	-1.581	0.21

* I : 14tonf-60km/h-15° , II : 14tonf-80km/h-15°
** long. acc. : longitudinal acceleration,
lat. acc. : lateral acceleration

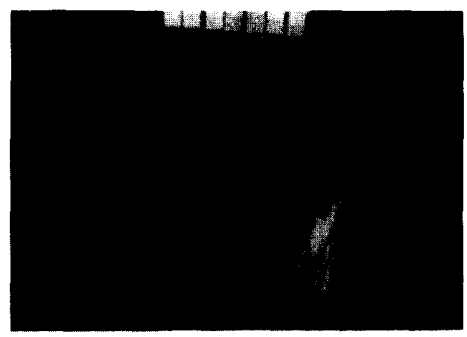

Fig. 2 Test Setup and Thrie-Beam Deflection After Testing

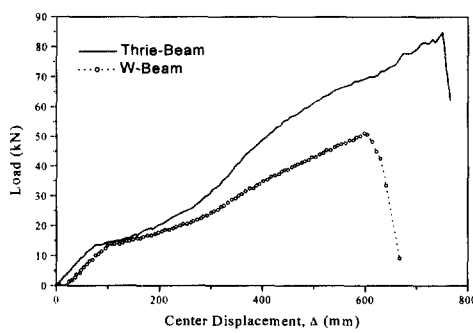

Fig. 3 Load - Deflection Relations at Beam Center

almost identical before beam stiffening occurs. From this discussion, it can be deduced that Type C barrier has larger strength and stiffness than Type B barrier.

In summary, all of the three barrier systems did not satisfy the requirement of structural adequacy for the barrier system of grade S. Type C barrier showed stiffer behavior than the others. Thus, the way to strengthen the installed Type C barrier will be experimentally investigated.

3. Static Tests for Posts

The methods to strengthen a barrier were deliberated as the following four categories; 1) adding members to existing structure, 2) replacing existing member with larger size member, 3) transforming existing member into composite member, and 4) increasing the degree of restraint that the footing provides to the post. To strengthen a barrier which was installed over a long distance, the strengthening method should be very simple and economical. Thus, first of all, the third and fourth categories, which are more economical method than the others, are experimentally investigated, and then the second one is studied. Since the contribution of post to the lateral stiffness of barrier system is much larger than that of beam, to escalate the efficiency of stiffness increase posts are considered to be transformed into composite member and to be a replacement.

Table 4 shows test matrix to evaluate the effect of the composite action of post and/or strengthening of footing on the increase of post stiffness. The composite posts are prepared by partially filling the inside of post with concrete to prevent local buckling of post after yielding near ground level. The partial filling of concrete is conducted from 30cm below ground level (GL-0.3), at which the top of inside soil is located, to 20 cm above ground level (GL+0.2). To strengthen the support of post concrete footing is cast around a post. The dimensions of concrete footing are a height of 0.5m and a diameter of 0.5m to have enough bearing strength and to prevent the movement of post. The 28 days compressive strength of concrete is f'_{ck} = 150kg/cm^2. Specimen A-1 shown in Table 4 is the same post as used in Type C barrier. All specimens except specimens D-1 and D-2 are installed to have the same penetration depth as that of the actual site. Figure 4 shows test setup. The horizontal force is applied by pile driver which makes it possible to keep the force applied horizontally.

Table 4 Static Test Matrix for Post

Test Article			Penetration Depth (m)	Loading Height (m)	Strengthening		
NO	Diameter (mm)	Thickness (mm)			Con'c Fill	Sand Fill	Con'c Footing
A-1	140	4.5	1.72	G.L.+1.08	×	×	×
A-2	140	4.5	1.72	G.L.+1.08	○	×	×
A-3	140	4.5	1.72	G.L.+1.08	×	×	○
A-4	140	4.5	1.72	G.L.+1.08	○	×	○
B-1	160	5	1.72	G.L.+1.08	×	×	×
B-2	160	5	1.72	G.L.+1.08	○	×	×
C-1	214	6	1.72	G.L.+1.08	×	×	×
C-2	214	6	1.72	G.L.+1.08	○	×	×
D-1	140	4.5	1.15	G.L.+0.6	×	×	×
D-2	140	4.5	1.15	G.L.+0.6	×	○	×

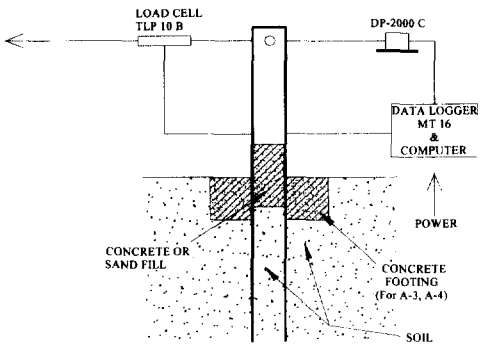

Fig. 4 Test Setup for Post

Fig. 5 Test Specimens After Testing.
(B-1, B-2, A-1, A-3, C-1, C-2 from left)

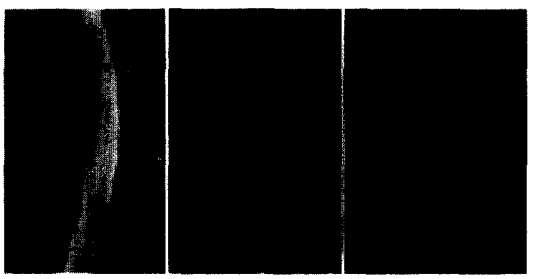

a) A-2 b) A-3 c) A-4

Fig. 6 Deformed Shape of Specimen A-2, A-3, and A-4

To check the compaction of the testing ground, plate bearing test was performed. Test field was a banked and well graded site for future construction. The settlement of it was believed to had been completed. Bearing index K_{30} at the time of 0.25cm settlement was 11.24kg/cm^2, which was less than the bearing index 20kg/cm^2 imposed for the banking area of asphalt pavement. Since the degree of compaction for the test site was less than the required one for the actual site, the lateral strength and stiffness of specimens under the condition of test site would be less than those of specimens under the condition of the actual site. The test results could be considered as to be conservative.

Failure modes of the test specimens after testing are presented in Figs. 5 and 6. Figure 5 shows the deformed shape of specimens B-1, B-2, A-1, A-3, C-1, and C-2. Specimen A-1 failed from the local buckling after yielding at 20cm below ground level. Concrete-filled steel post A-2 showed completely different failure mode. It showed large plastic flexural deformation without local buckling because concrete core restrained the local buckling of steel post (Fig. 6a). Specimen A-3 failed from the local buckling subsequent to yielding as specimen A-1 failed. However, it showed more brittle behavior than specimen A-1 because bearing stress due to concrete footing was applied to compressive side of post and the development of local buckling was accelerated. The deformed shape of concrete-filled steel post with concrete footing (specimen A-4) is shown in Fig. 6c. The failure mode of this specimen is the same as that of specimens A-1 and A-3. As far as failure mechanism was concerned, concrete core restrained local buckling while concrete footing accelerated local buckling.

The effects of concrete core and concrete footing on the behavior of steel post can be shown in Fig. 7. The elastic stiffness of post is 2.35 kN/cm, 2.54 kN/cm, 3.44 kN/cm, and 3.94 kN/cm for specimen A-1, A-2, A-3, and A-4, respectively. Concrete footing increased the elastic stiffness by 46% while concrete core increased it by 8%. When both concrete footing and concrete core were applied to strengthen the steel post, the elastic stiffness was increased by 68% as compared to that of steel post A-1. Concrete footing was more efficient in increasing the elastic stiffness than concrete core. The combination of concrete footing and concrete core yielded the largest increase of the elastic stiffness.

The ultimate strength of post is 20.6 kN, 35.3 kN, 21.6 kN, and 35.3 kN for specimen A-1, A-2, A-3, and A-4, respectively. Concrete core increased the strength by about 70% while the strength increase due to concrete footing is negligible. Due to the combination of concrete core and concrete footing the strength increase was the same as that due to concrete core. For specimen A-4, bearing stresses due to concrete footing caused premature bond failure between concrete core and steel post. The post-elastic behavior of specimen A-4 was more brittle than that of specimen A-2 due to concrete footing, and was more ductile than that of specimens A-1 and A-3 due to concrete core. For the combination of concrete core and concrete footing to get the same ductility as in the case of concrete core, the length of concrete core should be increased to obtain enough bond strength.

To investigate the behavior of larger post than that used for Type C barrier, specimens B-1, B-2, C-1, and C-2 were tested. Specimens C-1 and C-2 were too stiff and strong for the capacity of loading device to obtain the test results. The test results of specimens B-1 and B-2 are shown in Fig. 8. The elastic stiffness of post is 4.22 kN/cm and 4.83 kN/cm for specimen B-1 and B-2, respectively. Specimen B-2 yielded 14% larger elastic stiffness due to concrete core than specimen B-1. While the moment

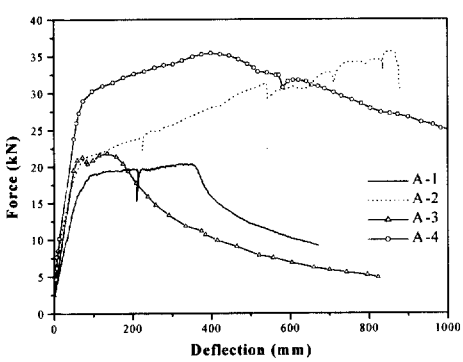

Fig. 7 Lateral Force-Deflection Relations for Specimens A-1, A-2, A-3, and A-4

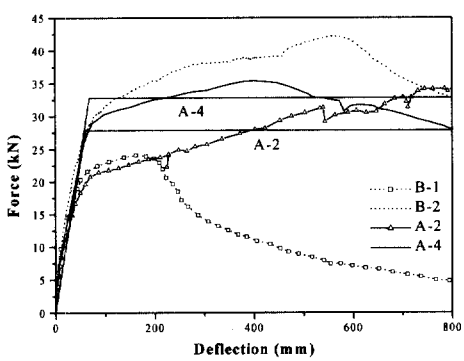

Fig. 8 Lateral Force-Deflection Relations for Specimens B-1, B-2, A-2, and A-4

of inertia of area for specimen B-1 was about 70% larger than that for specimen A-1, the elastic stiffness of specimen B-1 was 80% larger than that for specimen A-1. From the comparison of the elastic stiffness of specimens B-1 and A-4, it could be seen that the combination of concrete core and concrete footing yielded the similar efficiency to the 70% increase of second moments of area in increasing the stiffness.

The ultimate strength of post is 24.5 kN and 42.1 kN for specimen B-1 and B-2, respectively. The strength of B-2 was 70% larger than that of B-1 due to concrete core as in the case of specimens A-1 and A-2. The post-elastic behavior of specimen B-2 was more ductile than that of specimen B-1 due to concrete core, and was more brittle than that of specimen A-2. For concrete-filled steel posts to obtain a uniform ductility regardless of the size of post, the variation of the bond strength according to the length of concrete core for various sizes of post should be investigated.

The ultimate strength of specimens A-2 and A-4 is much larger than that of specimen B-1 even though the plastic section modulus of B-1 is 45% larger than that of steel post of specimens A-2 and A-4. The load-deflection curves of A-2 and A-4, as shown in Fig. 8, could be idealized as an elastic-perfectly plastic one making the area under the idealized curve equal to that under the original graph[3]. From the idealized curves, the ultimate strength is 27.44 kN and 32.34 kN for A-2 and A-4, respectively. Considering that the plastic hinge occurred at 19cm below ground level, the plastic moment could be determined from multiplying the ultimate strength by the distance (1.08+0.19=1.27m) between the loading point and the location of plastic hinge. Thus, the resulting plastic moment was 3,485 kN-cm and 4,107 kN-cm for specimen A-2 and A-4, respectively. From the comparison of these moments and the plastic moment of A-1, it could be seen that the strengthening methods of A-2 and A-4 were equivalent to increasing the plastic section modulus by 40% and 65%, respectively.

Figure 9 shows the results of specimens D-1 and D-2. The specimens seem to have quite high yield strength. However, considering their loading point(GL+0.6m instead of GL+1.08m), it can be found that they do not have larger yield strength than specimen A-1. From the performance of sand-filled post D-2, it can be seen that the composite action can not be achieved without bond strength between filling materials and steel post as expected.

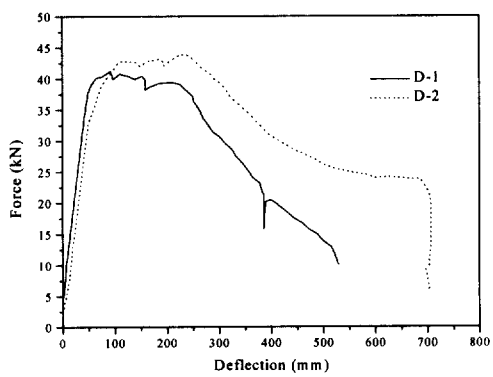

Fig. 9 Lateral Force-Deflection Relations for Specimens D-1 and D-2

In summary, the strengthening methods of specimen A-2 and A-4 were very effective way to strengthen a post. Simply casting concrete footing around the existing post (A-3) might worsen the situation. The strengthening method of A-4, which was the combination of A-2 and A-3, was more effective than that of A-2 which partially filled concrete inside a post. But, from the viewpoint of construction the strengthening method of A-2 would be preferred one.

4. Final Evaluation by Barrier Ⅶ

To strengthen the installed Type C barrier various strengthening methods were investigated. The strengthening methods of partially filling concrete inside a post(A-2) and concrete-filling with concrete footing (A-4) were effective to increase the stiffness, the strength, and the ductility of a post. Since the strengthening method of A-2 is more economical than that of A-4, the former is first investigated. The latter, if needed, will be investigated. To evaluate the impact performance of Type C barrier system strengthened by the method of A-2, simulations for the resulting barrier system were conducted for the impact condition of 14tonf-80km/h-15° using Barrier Ⅶ.

The post properties used for the Barrier Ⅶ simulations are shown in Table 5 and they are the values obtained from the idealized curve in Fig. 8. The elastic stiffness of post presented in Table 5 were the modified one to account for the difference between the loading point(108cm) and the height at which a main beam is located (60cm). The deflection at failure shown in Table 5 was calculated to correspond to the energy under the actual curve in Fig. 8.

Simulation results for Type C barrier system strengthened by the method of A-2 are presented in Fig. 10 to 12. Figure 10 shows the deflection shape of the strengthened Type C barrier at each 0.05s interval for the impact condition of 14tonf-80km/h-15° . Figure 11 shows the deflection shape of the original Type C barrier for the same impact condition. These two figures highlight how the posts strengthened by filling concrete increase the overall stiffness of Type C barrier system. For the strengthened Type C barrier, the maximum dynamic deflection was 38.5in(98cm) at 0.65s, which was smaller than the deflection limit of 1.1m used for the assessment of structural adequacy. Figure 12 shows the longitudinal and lateral acceleration of the vehicle for the impact condition of 14tonf-80km/h-15° against Type C barrier strengthened by the method of A-2. Maximum deceleration (negative acceleration) was -0.92g at 0.4s and -2.09g at 0.25s, in the longitudinal and the lateral direction, respectively. These maximum values satisfy the acceleration limit of 4g used for the assessment of occupant safety.

Thus, it is expected that Type C barrier system strengthened by partially filling concrete inside a post will satisfy the impact

Table 5 Section Properties of Strengthened Posts

Strengthening Method	Stiffness (kN/cm)	Yield Moment (kN-cm)	Deflection at Failure (cm)
A-2	10.5	3,485	76

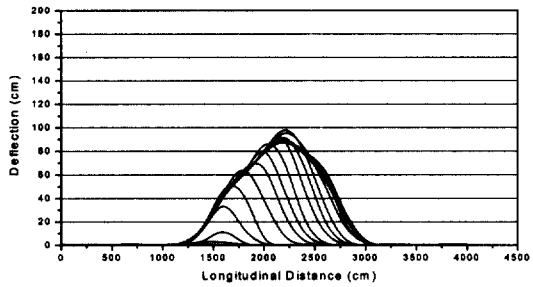

Fig. 10 Deformed Shape of Strengthened Type C Barrier

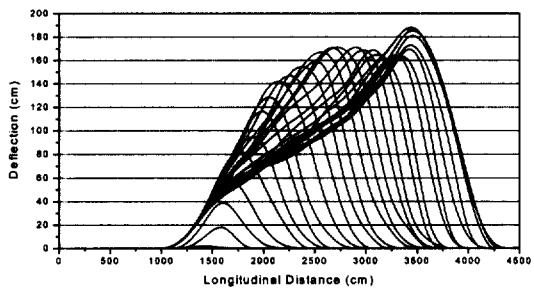

Fig. 11 Deformed Shape of Type C Barrier

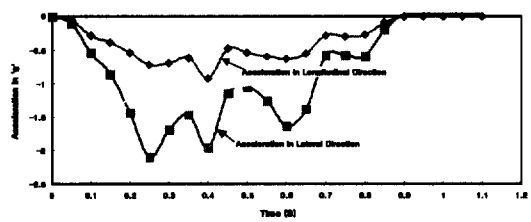

Fig. 12 Time-Acceleration Relations Against Strengthened Type C Barrier

performance criteria set forth for a specific danger area such as a highway region with which a railway runs in parallel.

5. Conclusion

To secure good visibility various steel barrier systems have been introduced in a specific danger area such as a road which runs in parallel with a railroad. None of the steel barrier systems was proven to satisfy the performance criteria set forth by Korea design guide.

From the simulation using Barrier Ⅶ, it was found that all of the steel barrier systems did not satisfy the requirement of structural adequacy for the barrier system of grade S. Type C barrier system showed stiffer behavior than the others. Thus, the way to strengthen the installed Type C barrier was experimentally investigated to satisfy the impact condition of 14tonf-80km/h-15° . The strengthening methods of partially filling concrete inside a post (A-2) and concrete-filling with concrete footing(A-4) were effective to increase the stiffness, the strength, and the ductility of the existing post. The impact performance of Type C barrier system strengthened by the method of A-2 was investigated for the impact condition of 14tonf-80km/h-15° by using Barrier Ⅶ. It was found that Type C barrier system strengthened by partially filling concrete inside a post would satisfy the impact performance criteria set forth for a highway region with which a railway runs in parallel.

REFERENCE

1. "Installation and Maintenance Guide for Roadside Safety Appurtenance: Longitudinal Barrier," Ministry of Construction and Transportation, Rep. of Korea, 1997.
2. Powell, G.H. BARRIER VII: A Computer Program for Evaluation of Automobile Barrier System, Report FHWA RD-73-51, FHWA, U.S. Department of Transportation, April 1973.
3. J.F.Dewey, J.F. Jeyapalan, T.J. Hirsch,

and H.E. Ross, "A study of the Soil Structure Interaction Behavior of Highway Guardrail Posts," Res. Report 343-1, Texas Transportation Institute, Texas A&M University, College station, Texas, July 1983.

4. H.E. Ross, Jr., D.C. Sicking, R.A. Zimmer, and J.D. Michie, "Recommended Procedures for the Safety Performance Evaluation of Highway Features," NCHRP Report350, Transportation Research Board, Washington, D.C., 1993.

5. Ray, M.H., "Evaluation of Design Analysis Procedures and Acceptance Criteria for Roadside Hardware," Report FHWA RD-87-097, FHWA, U.S. Department of Transportation, August, 1987.

6. PWRI, "Research for the Development of High Performance Steel Barrier," Report No. 94, Traffic Safety Division, PWRI, Ministry of Land, Infrastructure and Transport, Japan, 1993.

(접수일자 : 2001년 5월 17일)